

Optic flow based AFCS for rotorcraft automatic manoeuvring (terrain following, take-off and landing)

Franck Ruffier and Nicolas Franceschini
Biorobotic Research Group, Movement and Perception Lab.,
CNRS / Univ. de la Méditerranée
31, chemin Joseph Aiguier, 13402 Marseille Cedex 20, FRANCE
{ruffier, franceschini}@laps.univ-mrs.fr

Winged insects were solving obstacle avoidance, odometry and navigation problems long before there were any humans on Earth. Insects' guidance principles could therefore be harnessed for serving the field of aeronautics. At our laboratory, we have long seen winged insects as valuable model systems for building dynamic stabilization and guidance systems into artificial micro-flyers [3-5].

We have developed a visually based autopilot which is able to make a miniature rotorcraft automatically cruise and follow terrain [9]. We built a proof-of-concept, tethered robot that flies indoors over an environment composed of contrasting features randomly arranged on the floor. We show the feasibility of a visuomotor control loop that acts upon the thrust so as to maintain the optic flow (OF) estimated in the downward direction to a reference value. The OF sensor is an Elementary Motion Detector (EMD) [24, 8], the functional structure of which was inspired by those of the housefly, which were previously investigated at our Laboratory by performing electrophysiological recordings while applying optical microstimuli to single photoreceptor cells of the compound eye [13].

We show that this vision based autopilot, which we have called OCTAVE (Optic flow Control sysTem for Aerial Vehicles) is also able to control risky manoeuvres such as take-off and landing, while reacting appropriately to wind disturbances [35]. All these reputedly demanding tasks are performed *with one and the same visuomotor control loop without any need for an explicit knowledge of ground speed, air speed, descent speed and height over terrain*. The non-emissive sensor and simple processing system are particularly suitable for use with MAVs, whose avionic payload is only a few grams. But the OCTAVE autopilot could also contribute to relieve a remote operator from the lowly and difficult task of continuously piloting and guiding a larger UAV. Likewise, it could provide guiding assistance to manned aircraft*.

Keywords - UAV (Unmanned Aerial Vehicle), MAV (Micro-Air Vehicle), AFCS (Automatic Flight Control Systems), optical flow (OF), Biorobotics, Bionics, Biomimetics

*Patent Pending

I. INTRODUCTION

The biorobotics approach developed at our laboratory since 1985 [1-10] has led to designing and testing robots which process similar cues to those used by insects in real life. When building autonomous flying machines weighing hardly 100 grams, taking a look into natural autonomous fliers such as birds, chiroptera and winged insects can suggest some interesting solutions to the problems arising on this tiny scale. Winged insects were solving obstacle avoidance, odometry and navigation problems long before there were any humans on Earth, and we have good reason, to believe that their guidance principles could provide roboticists with innovative ideas. Winged insects have been known for 64 years to react visually to the apparent movement of the ground caused by their own bodily motion [11]. Surprisingly, this natural visual cue, which has been called the “*optic flow*” (OF), has not pervaded the field of aerospace engineering yet, although many data have been gleaned about the sensors and circuits that process the OF in the insect eye [12-14, 31].

Conferring some autonomy and authority upon an aircraft, especially during take off and landing or in the presence of wind disturbances, is a challenging task. It involves many issues such as mass, on-board energy and on-board processing resources required. Some of these issues have been addressed for large UAVs and drones using conventional computer vision systems [e.g., 15-17]. One particularly remarkable example is the R50 Yamaha helicopter developed by Amidi et al., which performed all its maneuvers (even the riskiest ones, such as hovering and landing) on the basis of natural visual landmarks and accurate sensor fusion [17]. Because of the heavy equipment required on-board this rotorcraft, the total airborne mass amounted to 67,000 grams. Building 1000 times lighter UAVs (in the 100-gram range) may require taking a different approach to the control systems, as several authors have attempted to do by turning to long-existing biological systems [3-10, 18-23]. Insect based visual flight control simulations have underlined the significance of the OF for autonomous agent navigation [3, 4, 18]. From careful behavioral

studies on honeybees' grazing landings, Srinivasan et al. proposed a landing strategy that consisted in maintaining a constant OF [19]. Then, 2 laws were formalized : (i) maintain a constant descent angle, (ii) adjust the forward flight speed so as to maintain a constant image angular velocity throughout the descent [20]. The authors reproduced these two laws first on a robotic gantry without dynamics [20]. More recently, Chahl et al. attempted to implement these two laws on a free-flying model aircraft to control its descent from 60 m down to 30 meters [21]. Ichikawa et al. addressed the problem of hovering with a 100-gram model helicopter using basic motion detection [22]. Altitude control and obstacle avoidance systems have also been tested recently on a free flying model plane [23].

At our laboratory, we have long seen winged insects as valuable model systems for building dynamic stabilization and visual guidance capacities into artificial micro-flyers [3]. In 1986, Franceschini et al. designed an optronic angular velocity sensors [24-25], the principle of which was based on the findings they had made on fly EMDs by performing electrophysiological recordings on single neurons while concomitantly applying optical microstimuli to single photoreceptor cells [13]. This velocity sensor evolved into a small (6-gram) analog circuit [26], which equipped, in particular, the fast obstacle avoiding "robot mouche" (robotfly) [2, 26]. Recently, we designed a lighter (0.8-gram) version of this EMD circuit combining analog and digital devices [8]. In the mid 90's, the same principle was taken up, independently, to design a smart VLSI circuit called the "facilitate and sample" velocity sensor [27]. In 1994, the Laboratory's first OF based altitude control simulation studies were published [3]. Netter and Franceschini's simulated an OF based terrain following behavior [4-5] with a forward looking 20 pixel-retina (the latter simulation was recently confirmed using a similar eye, looking down in the same way, over a similar environment [28]). Their results also showed that OF based landing was possible by linearly decreasing the rotorcraft forward speed while maintaining a reference OF [4]. The authors constructed a tethered 850-gram helicopter which was able to jump over an obstacle on the basis of its 19 EMDs [5]. Biologically inspired microrobotics also led to the development of a new EMD-based visual sensor called OSCAR, which enables a 100-gram tethered MAV to robustly perform tasks such as visual fixation and tracking, even in the presence of various disturbances [6, 10].

In a previous paper [9], we described a rotorcraft capable of effective terrain-following, designed on the basis of a simple, vision-based Automatic Flight Control System (AFCS). We showed that the AFCS, called OCTAVE (Optic flow Control system for Aerospace Vehicles) enabled a minimalistic optronic system to guide an aerial vehicle automatically on the basis of visual cues, without any need for a remote pilot to take the responsibility for carrying out the ground avoidance

task himself or herself. The remote pilot (or an onboard system having some authority) was simply required to set: (i) a pitch angle and (ii) an OF set point. These two parameters determined the height at which the robot flew above the ground in the absence of wind disturbances. For a given OF reference, any change in the ground speed (occurring for whatever reason) automatically led the aircraft to ascend or descend.

The present results extend these findings to three reputedly difficult tasks for an autonomous aerial robot: autonomous take off, autonomous landing and autonomous compensation for wind disturbances. In section 2, we describe the insect based visual guidance principle adopted. Section 3 focuses on the experimental setup used to test this principle on a tethered Micro-Air Vehicle. In section 4, we describe the autonomous terrain following, autonomous take off, autonomous landing and autonomous performances of the aircraft with the presence of wind disturbances.

II. VISUAL GUIDANCE STRATEGY

A. Optic flow under pure translation over a terrain

An eye-bearing MAV flying in pure translation along the x -axis over an unknown terrain (Figure 1a) generates an elementary translational OF, ω :

$$\omega = \frac{v_x}{D} \sin \Phi \quad (1)$$

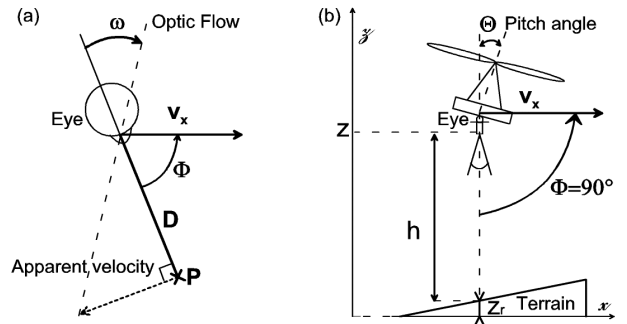


Figure 1. (a) An eye translating at velocity v_x over a contrast point P located at distance D and elevation Φ generates an angular retinal velocity ω . (b) A micro-helicopter pitched forward by an angle θ flies at groundspeed v_x in the absence of wind. As the gaze direction is maintained vertically downwards ($\Phi=90^\circ$), D becomes h , the distance above the terrain.

where v_x is the speed (ground speed) of the aircraft with respect to the ground, D its distance from the ground and Φ the angle between the gaze direction and the horizontal heading direction.

The OF generated is very small around the direction of self-motion ($\Phi = 0^\circ$), which is a pole of the OF field. The largest OF occurs at an angle of 90° from the pole. As we will see latter, we keep the robot's eye oriented downwards ($\Phi=90^\circ$) so that D becomes the height h with respect to the

ground (Figure 1b). Under these conditions, the OF range is maximized and w is simply the quotient of the ground speed \mathbf{v}_x and the height h .

$$\omega = \frac{v_x}{h} \quad \text{when } \Phi = 90^\circ \quad (2)$$

B. Bio-inspired OCTAVE principle

The guidance strategy proposed here is inspired by observations made by Kennedy more than 50 years ago on the flight behavior of mosquitoes [11] and migrating locusts [29]. Locusts' behavior would consist in maintaining a steady retinal angular velocity. Upon analyzing the flight of the free-flying fruitfly (*Drosophila*), David noted the existence of a relationship between flight speed and body angle [30]. The direction of the thrust generated by the two wings is mainly governed by the body pitch angle. The horizontal component of the thrust (i.e., the propulsive force, which causes the forward motion and determines the flight speed) therefore depends on the body pitch angle as well. Pitch angle and thrust are also the key parameters in the OCTAVE autopilot that guides our miniature rotorcraft. The thrust vectoring mode we use, which consists in controlling only the direction (body pitch angle) and the magnitude of the thrust on the rotorcraft, is comparable to the propulsion mode used by the fruitfly.

C. OCTAVE visuomotor control loop

The OCTAVE Automatic Flight Control System (AFCS) operates by *regulating the OF* (Figure 2). This strategy differs from the other strategies classically used in aerospace research, such as pressure altitude servoing (by means of a barometer sensor) or ground height servoing (by means of a radio-altimeter sensor, for instance) or ground speed servoing (by means of a Doppler radar or laser velocimeter sensor, for instance). The essence of OCTAVE AFCS is to estimate neither the height h nor the ground speed \mathbf{v}_x but only the OF, which is the quotient of both variables.

The robot then reacts to variations in the OF by changing its thrust via the rotor speed (rotations per minute, *rpm*). Any increase in the OF (due to a decrease in the height h above the ground or to an increase of ground speed \mathbf{v}_x) causes the rotor *rpm* to increase (see the signs of the signals on the comparator, fig. 2, left) until a height h over ground is reached, which re-establishes the requisite OF. Both the relief and the wind speed are treated like "disturbances" which both affect the OF (Fig. 2). A rise in the relief or a stronger tail wind both immediately increase the thrust so as to raise the aerial robot above the ground until the OF estimation ω_{EMD} has decreased to the OF set point.

The visual control system described in Figure 2 is a simplified description of the complex dynamics of the visuomotor plus aero-mechanical system

processes at work. In our analysis of the visuomotor control loop, we focused on the travel and surge dynamics.

There are two main parameters to the OCTAVE autopilot:

1) The robot's pitch angle Θ (Fig.1, 2), which determines the direction of the rotor thrust.

The horizontal component of the thrust determines the air speed. By keeping the robot's pitch constant, and without the presence of wind, it is possible to keep the ground speed \mathbf{v}_x fairly constant, and the visuomotor control loop will thus interpret any variations in the OF as variations in the height h over the ground.

2) The OF set point, ω_{sp}

This parameter defines the ratio between the ground speed \mathbf{v}_x and the height h above the ground (equ. 2).

D. OCTAVE control loop implementation

The transfer function $\mathbf{G}_v(\mathbf{s})$ gives the surge dynamics between the pitch angle Θ [°] and the air speed \mathbf{v}_a [m/s]. $\mathbf{G}_z(\mathbf{s})$, the heave dynamics transfer function, was identified under the present experimental conditions from the response to a step input. $\mathbf{G}_z(\mathbf{s})$ gives the linear transfer between the DC motor control signal \mathbf{u} [V] around the operating point and the altitude, \mathbf{z} [m].

$$G_z(s) = \frac{Z(s)}{U(s)} = \frac{K_z \omega_z^2}{s^2 + 2\xi_z \omega_z s + \omega_z^2} \quad (3)$$

with $K_z = 1.114 \text{ m/V}$, $\xi_z = 0.2239$ and $\omega_z = 0.9511 \text{ rad/s}$

A lead controller $\mathbf{C}_\omega(\mathbf{s})$ was introduced into the feedback loop to increase the phase margin and the damping, and thus to improve the stability and to decrease the response overshoot. The controller also includes a low-pass filter, which reduces the effects of short time errors on the OF estimation and smoothes the jumpy control signal at the time of a new OF update. This low-pass filter suitably decreases the jitter in the rotor control signal. The overall OF controller $\mathbf{C}_\omega(\mathbf{s})$, which runs on-line on a dSpace DSP board, is :

$$C_\omega(s) = K_c \left(\frac{\tau_1 s + 1}{\tau_2 s + 1} \right) \left(\frac{1}{\tau_3 s + 1} \right) \quad (4)$$

with $K_c = 0.2592 \text{ V.s/rad}$, $\tau_1 = 1.5\text{s}$, $\tau_2 = 0.12\text{s}$, $\tau_3 = 0.25\text{s}$

First, we checked that the controller is robust to parametric variations in the 1 to 3m/s ground speed range and in the 0 to 2m altitude range in the absence of wind disturbances. The system includes various couplings. The gain \mathbf{K}_z was found to depend in a range of $\pm 50\%$ both on the rotor control signal (increasingly) and on the speed (decreasingly). The pulsation ω_z and the damping

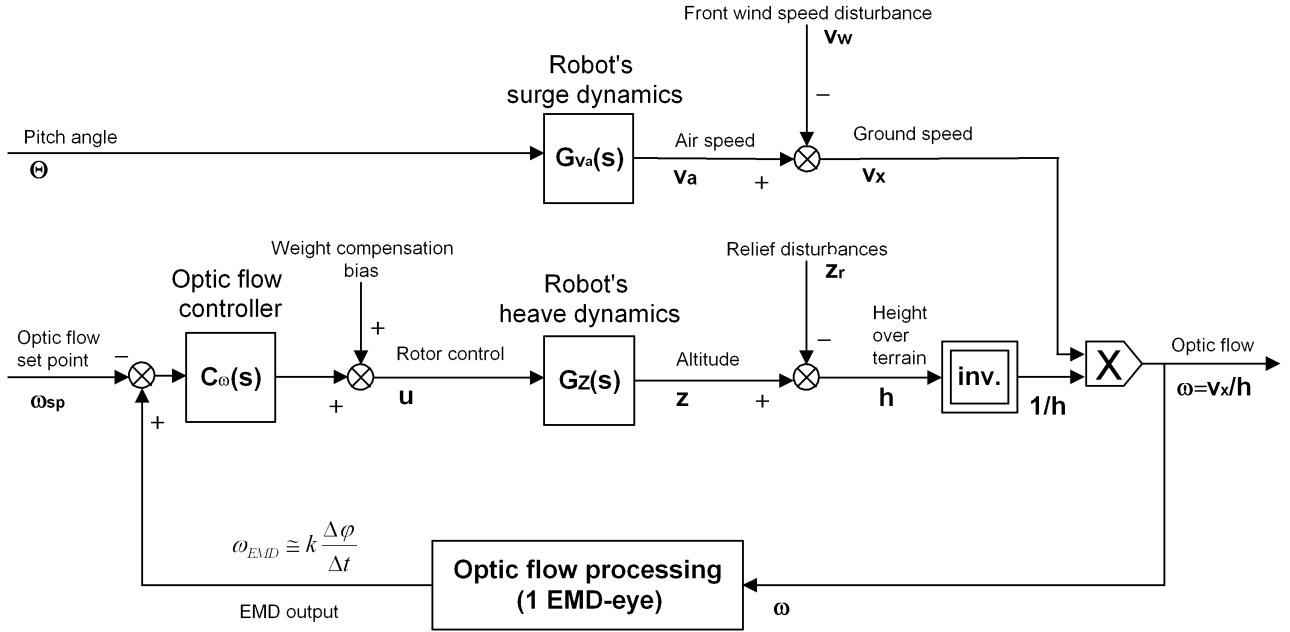


Figure 2. The OCTAVE autopilot controls two inputs on the robot's dynamics: the direction of the thrust, which eventually determines the groundspeed v_x , and the amplitude of the thrust, which eventually determines the altitude z . In the results presented in this paper, the thrust direction is set at a constant value while the thrust magnitude results from the OF regulation. The OF controller $C_\omega(s)$ which we incorporated into the loop regulates the OF ω measured by an EMD circuit. When the EMD output ω_{EMD} is higher than the OF set point ω_{sp} , $C_\omega(s)$ commands a higher rotor *rpm*. This leads to an increase in altitude, which induces a decrease in OF. The ground speed v_x directly depends on the helicopter pitch angle. The ground speed v_x can be said to weigh the OF according to equ. (2).

factor ξ_z vary to a lesser extent. We neglected the coupling between the rotor control signal, u [V], and the airspeed, v_a [m/s]: our experimental data attested that this coupling is weak (the speed remains fairly constant, Figure 4b).

A local rotor speed control loop (not shown in Fig. 2) was used to improve the dynamic properties of the overall visuomotor control system. This control loop counteracts any local aerodynamic disturbances impinging on the rotor. At low rotor control signal values, the MAV stays at altitude zero until a lift threshold is reached that equals for its weight. This “dead zone” is counterbalanced for by adding a bias to the rotor control signal (see Figure 2).

For the mean of convenience, a I/O DSP board (see Section 3B) hosted the control system which is running at 1kHz and is composed of a few filters and summation elements. This control system simplicity should allow its implementation onboard a tiny 8-bit microcontroller.

E. Bio-inspired OF processing

The OF processing is carried out by two devices:

1) An elementary eye, which transforms the OF ω generated by the robot's forward motion into a time lag Δt between the responses of two neighboring photoreceptors: Δt is an inverse function of ω (equ. 5). The two photoreceptor optical axes are separated by an angle $\Delta\phi$.

2) An insect-based Elementary Motion Detector (EMD) which processes this time lag Δt in a nonlinear way to provide the OF estimation ω_{EMD} according to :

$$\omega_{EMD} \cong k \frac{\Delta\phi}{\Delta t} = k\omega \quad (5)$$

The responses of this velocity sensor are monotonic with respect to the OF, unlike the responses of correlation based EMDs [31]. Our current hybrid implementation of an EMD, which combines both analog preprocessing and digital microcontroller-based processing, is a small module weighing only 0.8-gram [8], which lends itself easily to being mounted on-board the aerial robot. However, the robot's performances described here (Section 5) were obtained with an EMD circuit based on a *Field Programmable Analog Array* (FPAA by Anadigm), which was conveniently placed off-board [8].

III. EXPERIMENTAL SET-UP

A. Aerial robot

We built a small (100-gram) rotorcraft consisting of a rotor, a miniature electronic eye and its control electronics (Figure 3a). This “micro-air vehicle” (MAV) was based on the rotor mast of the Keyence “Revolutor” RC model helicopter. For the sake of experimental convenience, we added a landing gear ($l = 0.3m$) which extends below the

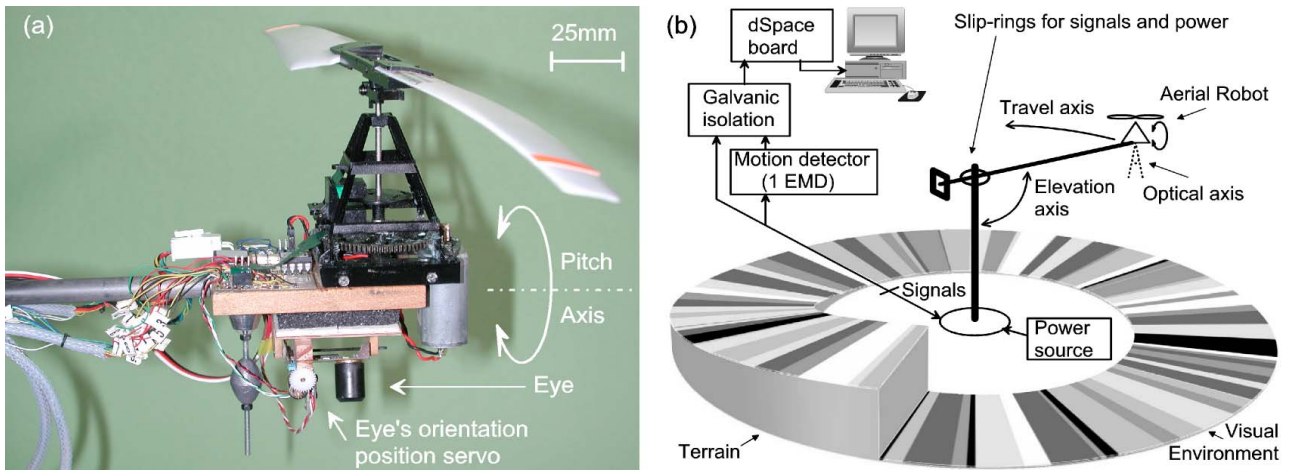


Figure 3. a) 100-gram rotorcraft developed for testing the OF autopilot. A PWM-controlled DC motor drives the 30-cm diameter, 5-gram propeller via a reducer. The robot can be oriented around its pitch axis by means of an external signal. The electronic eye is mounted on a thin PCB, the pitch of which is controlled by a 2.4g position servo system. When the robot pitch angle changes, the micro-servo counterrotates the eye so as to keep the gaze oriented vertically downwards, as shown in figure 1b. b) Test-rig composed of a pantographic whirling arm supporting the 100-gram rotorcraft which flies over a 4.5-meter outside diameter arena. The textured terrain below consists of randomly distributed, variously contrasting sectors. A ramp which stops abruptly at the height of 50 cm was added to one third of the arena to test the robot's reaction to terrain output disturbances (section IV-A).

robot's eye. The altitude plotted (section IV) therefore corresponds to $z-l$, the altitude of the wheels.

B. Test-rig

The rotorcraft is tethered to the end of a light, counterbalanced and pantographic whirling arm (Figure 3b) [4, 5], which is driven in elevation and azimuth by the aircraft's lift and propulsive forces, respectively. Any increase in the rotor rpm causes the aerial robot to lift and rise. Any forward tilting of the rotor by a few degrees causes the robot to move forward (while decreasing the lift). The mean circumference of the path traveled by the MAV during one lap is about 12 meters. For the sake of convenience, we decided to plot the trajectories (section IV) on a two dimensional plane defined by the altitude and the horizontal distance traveled.

A computer printed disc (outer diameter 4.5-meter) was laid on the ground to simulate a richly contrasting environment containing randomly ordered contrasting sectors. The various sector widths correspond to a ~ 30 -fold spatial frequency range (from 0.06 to 1.75 cycles per degree, for $h = 1$ m), which is a suitable range for testing the robustness of the visual processing system. As measured in the same (near IR) spectral range as that of interest in the robot's eye (whose sensitivity peaks at $\lambda=850\text{nm}$), the effective edge contrast turned out to be relatively low (from 4% to 30%) on the printed disc.

A PC equipped with an input/output DSP board (dSpace) coupled with MATLAB/Simulink was used to run the experiments in real time (without depending on the PC operating system), while monitoring the robot's behavior with a couple of ground-truth sensors (a servo-potentiometer on the elevation axis and an optical encoder on the travel axis). The experimenter remotely commanded the

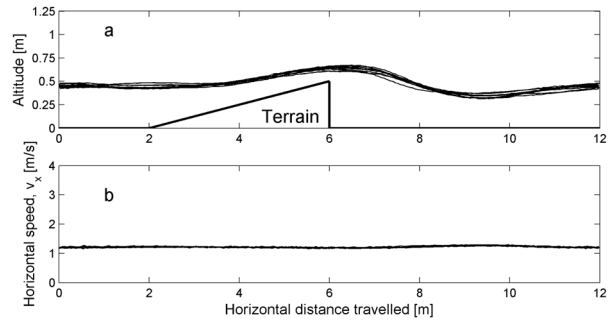


Figure 4. Automatic terrain following under visual control. The record shows 10 consecutive trajectories during which the robot covered a distance of 120 m in 100 seconds at a speed of 1.2m/s without ever crashing. The OCTAVE autopilot gives reproducible, reliable results in the context of a terrain following task.

servo-motor pitching the aerial robot forwards to attain the required speed.

This test-rig with a tethered MAV enabled us to reliably and reproducibly test the performances of the OCTAVE autopilot under safe conditions.

IV. EXPERIMENTAL RESULTS

All the experiments were first run in simulation using the same ground texture as that used during the present experimental tests, but only the real physical tests are presented here.

A. Automatic terrain following

Part of the visual environment was mounted on a slanted surface (a 7° angle "circular ramp"). This relief creates a serious output "disturbance" in the OCTAVE loop (see Fig. 2) whose efficiency can therefore be tested.

The robot's altitude (Figure 4a) was monitored during ten cycles of travel over the scene depicted in figure 3 and the trajectories recorded showed

that the robot automatically followed the terrain smoothly and reproducibly in spite of the presence of aerodynamic disturbances such as ground effects and air turbulence. The OCTAVE autopilot gives reliable results despite the complex dynamics of the overall system (visuo-motor system + aeromechanical system + test-rig). The whirling arm gives rise to additional inertia but negligible friction.

The OCTAVE autopilot thus causes the robot altitude to vary automatically as required by the changing relief of the land. Interestingly, the use of this OF regulation automatically generates a “safe height”, although no explicit knowledge about the ground speed, descent speed or the height above the ground is available on-board the vehicle. A detailed analysis of these trajectories was presented previously [9]. In particular, we established that the robot followed the terrain smoothly at heights depending on the OF set point. We showed the fine structure of the OF signal which the OCTAVE controller attempts to maintain at the reference value. We also established that the “safe height” conveniently increases with the ground speed: the faster the robot is moving, the further away from the obstacles it will fly [9].

B. Automatic take off

In all the subsequent experiments, the ground obstacle (ramp) was removed from the test-rig so that the ground remained flat.

To initiate an automatic take off, the idea is to pitch the MAV body “nose down” gradually so as to gradually increase the horizontal speed v_x . The MAV is expected to then take off automatically because the OF controller will keep the ratio v_x/h constant at all times: if v_x increases, h must increase to maintain ω constant (equ. 2). Fig. 5 shows the results obtained using this strategy. By applying a ramp (duration 10 sec.) to the pitch control, the rotorcraft tilts forward gradually until reaching an inclination of 10° (pitch angle Θ in Fig. 2). As a result, the ground speed increases

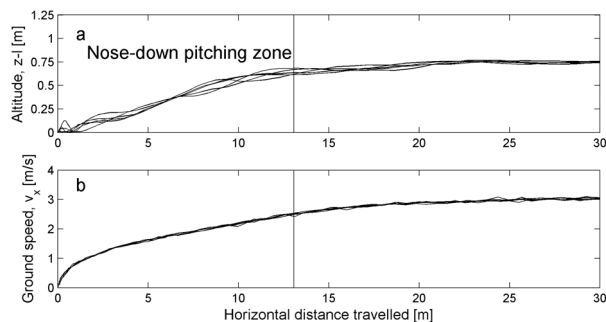


Figure 5. Automatic take off under visual control
First, the rotor speed is set to the levitation level (see weight compensation bias in Fig.2) and the OF loop is closed. Within the “nose down pitch zone”, the robot is tilted forward gradually, thereby increasing its air speed (b). This results in a smooth automatic take off controlled by the robot’s vision (a). With five tries, the OCTAVE autopilot was also found to produce reproducible take off trajectories.

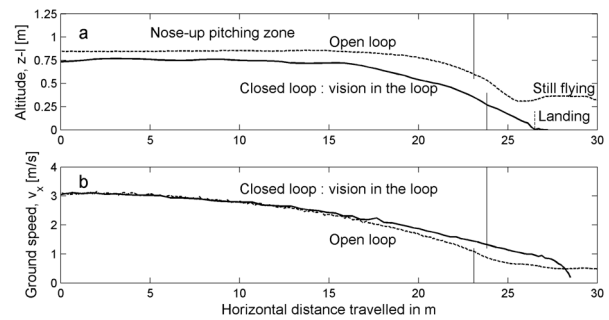


Figure 6. Automatic landing under visual control
Closed loop (solid line): A gradual rotor tilt “nose-up” triggers landing. The robot decelerates slowly (the inertia of the test-rig slows its deceleration). As the ground speed keeps decreasing (b), the height h over the ground (controlled by the OF autopilot) gradually decreases (a). This eventually results in a smooth landing at a ground speed close to zero. At touch down, the system cuts the gas.
Open loop (dashed line): the system does not manage to land.

continuously (Fig. 5b) and the rotorcraft is bound to gain height (Fig. 5a).

In Figure 5, five visually guided take off trajectories have been superimposed. The OF regulation loop makes the take off maneuvers highly reproducible. Again, the OCTAVE autopilot proved to be capable of a smooth altitude control.

C. Automatic landing

To effect a landing, the idea is to gradually raise the rotorcraft “nose up” so as to gradually decrease the horizontal speed v_x . The OF controller should do the rest, by:

- reducing the height with respect to ground so as to keep the ratio $v_x/h = \omega$ constant,
- eventually landing the rotorcraft, with a negligible forward speed at touchdown.

Fig. 6a gives the landing trajectories obtained under both closed loop and open loop conditions when the pitch angle Θ (see Fig. 2) was gradually reduced from 10° to 0° ramp-wise (10-second ramp). Under open-loop conditions, the MAV has difficulty in landing (Fig 6b : dashed curve) because, when approaching ground, a ground effect adversely increases the lift. By contrast, the MAV lands smoothly under closed loop conditions (Fig 6a: solid curve) and smoothly overcomes the

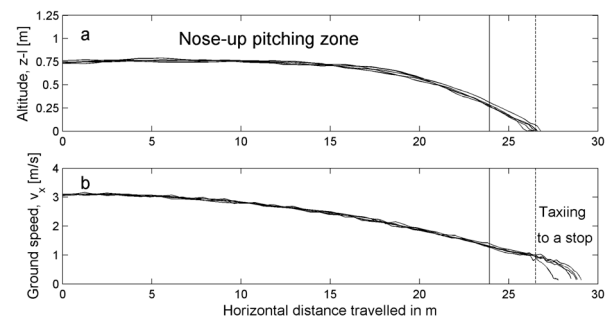


Figure 7. The miniature rotorcraft shows 5 very repetitive visually-guided landing trajectories. When the MAV touches the ground, the rotor is stopped and the mini-robot taxis to a stop, carried along by its own momentum.

complex ground effect.

The five visually guided landing trajectories superimposed in Fig. 7 show that the OF regulation makes for reliable and reproducible landing performances. Again, the OCTAVE autopilot always induced a smooth decrease in height. The time required for the robot to land depends on the tilting rate. But it also depends on the travel dynamics between the robot pitch angle and the ground speed (which here includes the test-rig inertia).

D. Automatic reaction to wind disturbances

In the last set of experiments, the course of the rotorcraft was disturbed by a head wind (produced by a fan) with a speed v_w of up to 1.5 m/s. As shown in Fig. 2, the wind speed constitutes a serious output disturbance, which interferes with the MAV airspeed and thus alters the ground speed. Under open loop conditions, the robot cannot overcome these output disturbances. Under closed loop conditions, however, a tail wind accelerates the MAV's ground speed and the OCTAVE autopilot reacts by automatically increasing the altitude to maintain the downward OF constant (result not shown here).

When there is a head wind, by contrast, the MAV inevitably loses speed (ground speed). The OCTAVE autopilot should respond in this case so as to automatically decrease the altitude, again maintaining a constant OF. This is exactly what is observed experimentally (Figure 8a-b, dashed lines: light head wind of ~ 0.5 m/s). Upon leaving the wind zone, the MAV is not slowed down by the wind any more, hence the ground speed increases and the robot responds by increasing the altitude since it cannot help keeping the OF at the set point (Fig 8a-b, dashed lines).

When facing a very strong head wind, the MAV's ground speed decreases so greatly that it tends to zero. This automatically triggers a *forced*

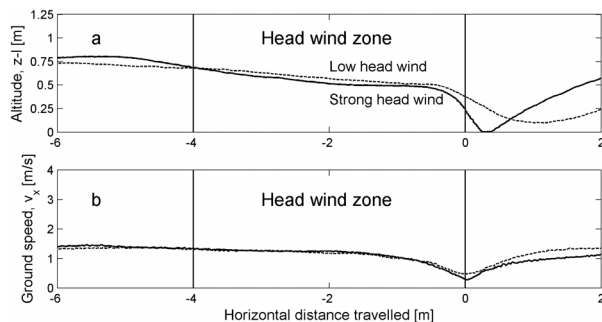


Figure 8. Copping with a head wind under closed loop conditions (dashed lines: low head wind $v_w \approx 0.5$ m/s; solid lines: strong head wind $v_w \approx 1.5$ m/s).

Head wind reduces the ground speed. The OCTAVE autopilot reacts by decreasing the height of the robot with respect to the ground. The stronger the wind, the lower the aerial minirobot flies, until landing at negligible forward speed (solid curves). In these experiments, a 30'20cm planar airfoil perpendicular to the travel axis was deliberately added to the MAV so that it would catch the wind, i.e., increase the drag.

landing which is all the safer since the ground speed is so low (Figure 8a-b, solid lines: strong head wind of ~ 1.5 m/s, landing speed ~ 0.3 m/s). At touch down, a haptic sensor in the landing gear could easily bring the lifting rotor to a halt. Since this was not done here, the robot immediately took off again after reaching the end of the front wind zone: again the height h over the ground naturally increased to match the naturally increasing ground speed and maintain the OF constant (Figure 8a-b, solid lines).

V. DISCUSSION AND CONCLUSION

In this study, we dealt with the reputedly difficult maneuvers that will have to be effected safely by the miniature unmanned aerial vehicles of the future. We have presented a quantitative study showing how a miniature 100-gram rotorcraft, equipped with an elementary optronic system, can take off automatically under visual control, hug the underlying terrain automatically, land automatically on command and react in a sensible way to unpredictable headwind or tailwind disturbances. The feasibility of OF based terrain following and landing was originally showed in simulations [4]. Another landing procedure [20] differs from the OF autopilot presented in this paper in that it requires the implementation of two control laws: maintaining a constant descent angle and maintaining a constant image angular velocity. By contrast, the OCTAVE autopilot presented here requires only an *optic flow regulation loop* whose controller acts upon the thrust amplitude exclusively, regardless of the vehicle's current forward groundspeed, airspeed or descent speed. We have shown that this single and simple *regulation loop* suffices to generate all the interesting behaviors mentioned above.

First, reliable terrain-following performances were obtained: OCTAVE suitably copes with the "disturbances" caused by an uneven relief and features such as a slanted ground by performing *terrain following*. The OCTAVE AFCS turned out to be robust and efficient within a given range of forward speeds (1 to 3 m/s). A "safe height" is generated automatically, which increases very conveniently with the ground speed [9]. Then we showed how the trajectory of the MAV in the vertical plane can be changed by simply altering the pitch angle, which determines the ground speed. Pitching the robot continuously nose-down and thereby increasing the ground speed causes the robot to automatically take off. Conversely, by tilting the robot progressively backward, the robot automatically loses height until it eventually alights. Hence, these apparently complex maneuvers are performed automatically in response to simple pitch commands.

When entering a head wind zone, the robot automatically reacted by flying lower : it decreases its height h with respect to ground, thereby

maintaining a “safe height” that matches its speed. This reaction (which might be problematic in the case of a passenger aircraft, but should be tolerable in UAVs and MAVs) actually occurs in nature. Reactions of this kind have been observed in both insects and birds. Migrating insects [29] and migrating birds [32] typically ascend under tail wind and descend when a lull occurs or when they come to face a light head wind. Whether it occurs in insects or birds or MAVs, this reaction is all the more sensible and ecological since a descending reaction to a head wind will bring them to less unfavorable winds at lower altitudes, leading to invaluable energy savings during their migration (insects, birds) or survey (MAVs).

Unlike most of the autopilots classically used in manned helicopters, the OCTAVE autopilot was not designed to provide the aerial robot with height holding or ground speed holding skills. It rather ensures that “OF holding” occurs so that the MAV will reach a “safe height” automatically at any speed. The main advantage of OCTAVE is that it ensures that any maneuvers and disturbance rejection will occur at all costs without collision with the ground: the result is measured in terms of task performances, and not in terms of metric variables (airspeed, height, etc.) usually measured on-board aircraft. The robot is able to take off, follow a shallow terrain, land and react to wind disturbances *although it is completely unaware of its airspeed, groundspeed, descent speed, height over the terrain and absolute altitude at any time*. In contrast with OCTAVE autopilot, classical AFCS operate relatively far from the ground. Automatic landing systems classically require *off-board* and bulky ground station ILS equipment. In the case of UAVs, they include items such as a radar that tracks the aircraft during its descent.

The use of a tether was essential here to be able to implement and test the basic strategy used: *OF regulation* on an elementary rotorcraft with limited (three) degrees of freedom. Tests on free-flying MAVs are more difficult to carry out and lack reproducibility: their results have tended to be more qualitative so far [21, 23], because a MAV will unlikely fly twice at the same height over the same site under the same wind disturbances. In our test-rig, however, the whirling arm introduces undesirable inertia into the control loop, which adversely affects both the heave and the surge dynamics: the robot is less agile than it would be if it were flying freely. On the other hand, a supporting tether facilitates the parameter monitoring and the understanding and tuning of the perception/action loop, while making the experiments more reproducible (see Figure 4, 5, 7). In any case, we considered that an incremental approach starting with a tethered vehicle and aiming at a free flying vehicle was essential to demonstrate the essence of the OCTAVE principle.

The system we have described here for the visual guidance of an aerial vehicle was inspired by the insect world, and the visual processing system

itself was inspired by the results of electrophysiological experiments carried out on living insects as well. Most present-day computer-assisted visual systems are not up to the task of guiding a 100-gram micro-air vehicle while meeting the drastic constraints consisting of a total avionic payload of less than 10 grams. Biologically inspired robotics can provide MAVs with well tried and tested alternative solutions, which in some cases are also scalable to larger UAVs. The non-emissive OCTAVE autopilot requires remarkably few resources. Its simple principle hints towards a *generic solution* to reputedly complex guidance problems which, as we showed here, can be solved by one and the same OF regulation loop. Once it has been further developed, the OCTAVE autopilot promises to afford MAVs, UAVs and full-sized aircraft greater decisional autonomy, and may also serve to assist human pilots. An OCTAVE autopilot equipped with an eye with a larger field of view could be implemented on-board free-flying 100-gram MAVs, where the body pitch and the eye pitch counter-rotation could be controlled by a micro vertical gyro. Since automatic take off, terrain following, ground collision avoidance and landing are also major issues for planetary [33] and submarine operations [34], the vision-based OCTAVE autopilot could also potentially be adapted to spacecraft, planetary vehicles, and benthic submarines.

ACKNOWLEDGEMENTS

We thank S. Viollet for his fruitful comments and suggestions during this work, S. Durand from Galatée Films for his data about bird migration, J. Serres for his comments on the manuscript, M. Boyron for his expert technical assistance, M. Rigal for the realization of the galvanic isolation of the dSpace board and J. Blanc for improving the English manuscript. This research was supported by CNRS (Life Science, Engineering Science, Communication and Information Science and Technology, Cogniscience, Microsystem and Microrobotic Programmes) and by an EU contract (IST/FET - 1999- 29043).

This paper is largely based on a paper entitled “Visually guided Micro-Aerial Vehicle : automatic take off, terrain following, landing and wind reaction,” by F. Ruffier and N. Franceschini appearing in Proceeding of the IEEE Int. Conf. on Robotics and Automation (ICRA 2004), pp. 2339-2346, April 26 - May 1 at New Orleans, USA.

REFERENCES

- [1] J-M. Pichon, C. Blanes and N. Franceschini, “Visual guidance of a mobile robot equipped with a network of self-motion sensors,” in Proc. of SPIE Conf. on Mobile Robots IV, W.J. Wolfe and W.H. Chun, Eds., Bellingham, U.S.A., 1989, SPIE Vol. 1195, pp. 44-53.
- [2] N. Franceschini, J.M. Pichon and C. Blanes, “From insect vision to robot vision,” Phil. Trans. R. Soc. Lond. B, 1992, 337: 283-294.

- [3] F. Mura and N. Franceschini, "Visual control of altitude and speed in a flying agent," in *From Animals to Animats III*, D. Cliff et al., Eds., MIT Press, Cambridge, U.S.A., 1994, pp. 91-99.
- [4] T. Netter and N. Franceschini, "Neuromorphic Optical Flow Sensing for Nap-of-the-Earth flight," in *Proc. of Conf. on Mobile Robots XIV*, D. W. Gage and H. M. Choset, Eds., Bellingham, U.S.A., 1999, SPIE Vol. 3838, pp. 208-216.
- [5] T. Netter and N. Franceschini, "A Robotic Aircraft that Follows Terrain Using a Neuromorphic Eye," in *Proc. of IEEE Conf. on Intelligent Robots and Systems (IROS)*, Lausanne, Switzerland, 2002, pp. 129-134.
- [6] S. Viollet, and N. Franceschini, "Super-accurate visual control of an aerial minirobot," *Proc. of Autonomous Minirobots for Research and Edutainment AMIRE*, U. Rückert, J. Sitte and U. Witkowski, Eds., Paderborn, Germany, 2001, pp. 215-224.
- [7] F. Ruffier, and F., Franceschini, N., "OCTAVE, système de contrôle bio-inspiré de l'altitude d'un micro-aéronef," *Actes des 1^{ères} journées du Réseau Thématique Pluridisciplinaire Micro-robotique*, CNRS, Rennes, France, 2002.
- [8] F. Ruffier, S. Viollet, S. Amic and N. Franceschini, "Bio-inspired optical flow circuits for the visual guidance of Micro-Air Vehicles," in *Proc. of IEEE Int. Symposium on Circuits and Systems (ISCAS)*, Bangkok, Thailand, 2003, Vol. III, pp. 846-849.
- [9] F. Ruffier, and N. Franceschini "OCTAVE, a bioinspired visuo-motor control system for the guidance of Micro-Air Vehicles," in *Bioengineered and Bioinspired Systems*, A. Rodriguez-Vazquez, D. Abbott, R. Carmona, Eds., Bellingham, U.S.A., 2003, SPIE Vol. 5119, pp.1-12.
- [10] F. Ruffier, S. Viollet and N. Franceschini, "Visual control of two aerial mini-robots by insect-based autopilots," *Advanced Robotics*, 2004 (In Press).
- [11] J.S. Kennedy, "The visual response of flying mosquitoes," *Proc. Roy. Soc. Lond. A*, 1940, 109:221-242.
- [12] K. Hausen and M. Egelhaaf, "Neural mechanisms of visual course-control in insects," *Facets of Vision*, D.G. Stavenga, R.C. Hardie, Eds., Springer, Berlin, 1989, pp. 391-424.
- [13] N. Franceschini, A. Riehle and A. Le Nestour, "Directionally Selective Motion Detection by Insect Neurons," *Facets of vision*, D.G. Stavenga, R.C. Hardie, Eds., Springer, Berlin, 1989, pp. 360-390.
- [14] T. Collett, H. Nalbach, and H. Wagner, "Visual stabilization in arthropods" in: *Visual motion and its use in the stabilization of gaze*, F.A. Miles, J. Wallman Eds. Elsevier, 1993, pp. 239-263
- [15] S. Furst, S. Werner, D. Dickmanns, and S. Werner, "Landmark navigation and autonomous landing approach with obstacle detection for aircraft," in *Proc. of SPIE AeroSense '97 Conf.*, Vol. 3088, Orlando FL, 1997, pp 94-105.
- [16] C.S. Sharp, O. Shakernia and S.S. Sastry, "A Vision System For Landing an Unmanned Aerial Vehicle," in *Proc. of IEEE Int. Conf. on Robotics and Automation (ICRA)*, Seoul, Korea, 2001, pp. 1720-1727.
- [17] O. Amidi, T. Kanade, and J.R. Miller, "Vision-Based Autonomous Helicopter Research at Carnegie Mellon Robotics Institute 1991-1997," in *Proc. American Helicopter Society Int. Conf. Gifu*, Japan, 1998.
- [18] T.R. Neumann and H. Bühlhoff, "Insect inspired visual control of translatory flight," in *Proc. of ECAL 2001*, Springer, Berlin, 2001, pp. 627-636.
- [19] M.V. Srinivasan, S.W. Zhang, M. Lehrer and T.S. Collett, "Honeybee navigation *en route* to the goal: visual flight control and odometry," *J. Exp. Biol.* 1996, 199:237-244.
- [20] M.V. Srinivasan, S.W. Zhang, J. Chahl, E. Barth and S. Venkatesh, "How Honeybees make grazing landings on flat surfaces," *Biological Cybernetics*, 2000, 83(3):171-183.
- [21] J.S. Chahl, M.V. Srinivasan and S.W. Zhang, "Landing Strategies in Honeybees and Applications to Uninhabited Airborne Vehicles," *Int. J. of Robotics Research*, 2004, 23 (2):101-110.
- [22] M. Ichikawa, H. Yamada and J. Takeuchi, "Flying robot with biologically inspired vision," *J. of Robotics and Mechatronics*, 2001, 13:621-624.
- [23] G.L. Barrows, C. Neely and K.T. Miller, "Optic flow sensors for MAV navigation," in *Fixed and flapping wing aerodynamics for Micro Air Vehicle applications*, *Progress in Astronautics and Aeronautics*, AIAA, 2001, Vol. 195, pp. 557-574.
- [24] N. Franceschini, C. Blanes and L. Oufar, "Passive, non-contact optical velocity sensor" (in French). *Dossier technique ANVAR/DVAR N°51 549*, Paris, 1986.
- [25] C. Blanes, "Appareil visuel élémentaire pour la navigation à vue d'un robot mobile autonome," Master thesis in Neurosciences ("DEA" in French), Neurosciences, Univ. Aix-Marseille II, 1986.
- [26] C. Blanes, "Guidage visuel d'un robot mobile autonome d'inspiration bionique," PhD thesis, Institut National Polytechnique de Grenoble, 1991.
- [27] J. Kramer, R. Sarpeshkar and C. Koch, "Pulse-Based Analog VLSI Velocity Sensors," *IEEE Trans. Circuits and Systems II*, 1997, 44:86-101.
- [28] W.C. Wu, L. Schenato, R. J. Wood and R.S. Fearing, "Biomimetic Sensor Suite for Flight Control of a Micromechanical Flying Insect: Design and Experimental Results," in *Proc. IEEE Int. Conf. on Robotics and Automation (ICRA)*, Taipei, Taiwan, 2003, pp 1146-1151.
- [29] J. S. Kennedy, "The migration of the desert locust (*Schistocerca gregaria* Forsk.)," *Phil. Trans. Royal Soc. B*, 1951, 235:163-290.
- [30] CT David, "The relationship between body angle and flight speed in free-flying *Drosophila*," *Physiol. Ent.*, 1978, 3:191-195.
- [31] W. Reichardt, "Movement perception in insects," in *Processing of Optical data by organisms and by machines*, W. Reichardt, Eds., New York: Academic Press, 1969, pp. 465-493.
- [32] T. Alestrom, *Bird Migration*, Cambridge University Press, 1990.
- [33] T. Kubota, T. Hashimoto and J. Kawaguchi, "Image Processing for Asteroid Exploration Mission MUSES-C," in *Proc. of IEEE 11th Int. Conf. on Advanced Robotics (ICAR)*, Coimbra, Portugal, 2003, pp. 1221-1226.
- [34] V. Creuze and B. Jouvencel, "Avoidance of Underwater Cliffs for Autonomous Underwater Vehicles," in *Proc. of IEEE Conf. on Intelligent Robots and Systems (IROS)*, Lausanne, Switzerland, 2002, pp. 793-798.
- [35] F. Ruffier and N. Franceschini "Visually guided Micro-Aerial Vehicle : automatic take off, terrain following, landing and wind reaction," in *Proc. of the IEEE International Conference on Robotics and Automation (ICRA 2004)*, New Orleans, USA, 2004, pp. 2339-2346.